

CMMHw3

Oliwia Lidwin

November 2, 2024

1 Oscillatory Motion and Chaos

The driving frequency can be approximated as 1, because the system's natural frequency ω_o is $\omega_o = \sqrt{\frac{g}{l}} \frac{rad}{s}$, where $g = 9.8 \frac{m}{s^2}$ and $l = 9.8m$. The formula used to derive the driving frequency Ω_d is

$$\Omega_D = \sqrt{\omega_o^2 - 2\gamma^2}$$

where $\gamma = 0.25s^{-1}$. Thus,

$$\Omega_D = \sqrt{1^2 - 2 * 0.25^2}$$

$$\Omega_D = \sqrt{0.875}$$

$$\Omega_D = 0.935 \frac{rad}{s}$$

The small-angle or linear approximation for a pendulum remains true when $\theta < 15$ degrees or 0.25 rad. If only considering the damping, it would be valid to assume the small angle approximation. However, there is also the driving amplitude, α_D , which is one of the factors in the driving force. Given that throughout this homework, the driving amplitude remains small, it would be valid to assume the small angle approximation holds. The goal of this exercise was to simulate a linear, damped, driven pendulum defined by either of the following

$$\frac{d^2\theta}{dt^2} = -\frac{g}{l}\theta - 2\gamma\frac{d\theta}{dt} + \alpha_D \sin(\Omega_D t)$$

$$\frac{d\omega}{dt} = -\frac{g}{l}\theta - 2\gamma\omega + \alpha_D \sin(\Omega_D t)$$

where $g = 9.8 \frac{m}{s^2}$, $l = 9.8m$, $\gamma = 0.25s^{-1}$, $\alpha_D = 0.2 \frac{rad}{s^2}$, and $\Omega_D = 0.935 \frac{rad}{s}$

Two methods were used to plot $\theta(t)$ and $\omega(t) = \frac{d\theta}{dt}$ until a steady-state solution was reached. These two methods were the Euler-Cromer and the Runge-Kutta 4th order methods. The appropriate plots are shown in Figure 1. Using the $\omega(t) = \frac{d\theta}{dt}$ curve, the amplitude, $\theta_o(\Omega_D)$, and phase shift, $\phi(\Omega_D)$ of the steady-state solution were extracted. The amplitude was found by taking the maximum of the steady-state solution of the Runge-Kutta $\omega(t)$ plot. The phase

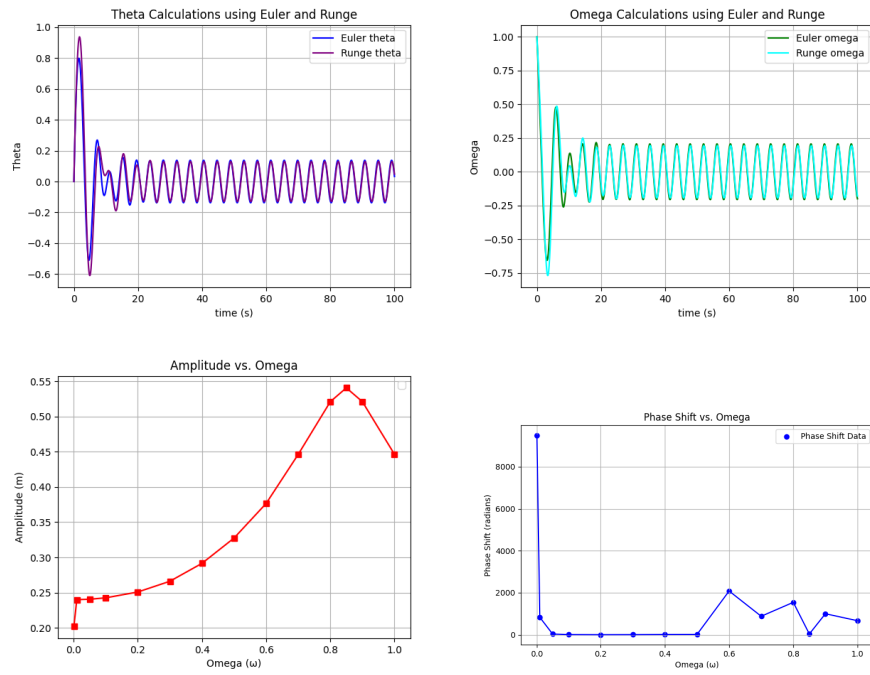


Figure 1: Euler-Cromer and Runge-Kutta 4th order methods for finding theta and omega(top) with amplitude trend and phase shift (bottom).

shift was found by taking the differences in time between the Euler-Cromer and the Runge-Kutta solutions.

From the amplitude, $\theta_o(\Omega_D)$, plot the full-width at half maximum of the resonance curve can be calculated. This was done by finding the peak of the curve at $\Omega_D = 0.85 \frac{rad}{s}$ with an amplitude of 0.54. This was then halved to look for $\theta_o(\Omega_D) = 0.27$. The the left hand side of the curve has a value of $\theta_o(\Omega_D) = 0.27$ at about 0.38. The amplitude curve should be symmetric, so the distance from the left hand side of the curve to the middle at $\Omega_D = 0.85 \frac{rad}{s}$ should be equivalent to the distance from the middle of the curve to the right hand side of the curve such that $\theta_o(\Omega_D) = 0.27$. If the difference from the left to the center is $0.85 - 0.35 = 0.50$, then the $\Omega_D = 0.85 + 0.50 = 1.35$ on the right side. The distance from the left side to the right side is a total of 1, which is equal to $4 * \gamma = 4 * 0.25$.

Using the $\theta(t)$ and $\omega(t) = \frac{d\theta}{dt}$ with $\Omega_D = 1$, the potential, kinetic and total energy of the Runge-Kutta method were calculated. The mass was not specified and was irrelevant to the purpose of this analysis. The potential energy was calculated by doing $E_p = mgl(1 - \cos \theta)$. The kinetic energy was calculated by doing $E_k = 0.5ml^2\omega^2$. The total energy was the addition of the potential and kinetic energy $E_t = E_p + E_k$. Figure 2 shows the energy of the system as a function of time. The energy plot is determined by the equilibrium from the driving and dampening force.

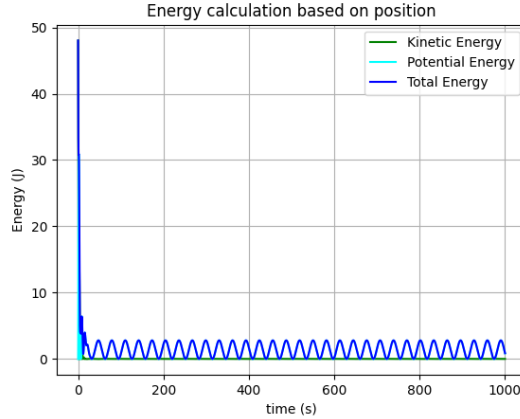


Figure 2: Kinetic, Potential and Total Energy using Runge-Kutta 4th order. Pendulum reaches steady state.

The system has been assumed to be linear, but will now be assumed to be non-linear by replacing θ with $\sin \theta$ in the restoring force term $-\frac{g}{l}\theta$. The result was plotted using the Runge-Kutta 4th order method and is recorded in Figure 3. This plot clearly shows more instability than those of Figure 1. This may be the case due to no longer using the small angle approximation.

The non-linear approach was used with $\Omega_D = 0.666s^{-1}$ and $\alpha_D =$

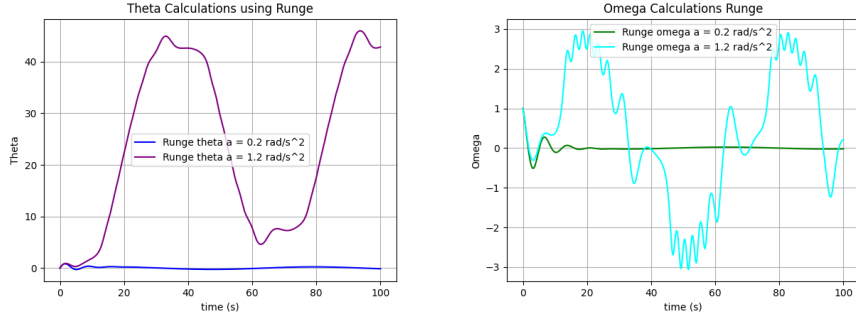


Figure 3: Euler-Cromer and Runge-Kutta 4th order methods for finding theta and omega(top) of non-linear effect.

0.2, 0.5, and $1.2 \frac{rad}{s^2}$ to compute the difference in simulation with initial angles that differ by 0.001 rad. The difference in the plots was graphed and are shown in Figure 4. The logarithm of the difference in simulation vs. time was plotted and a trend line was drawn such that the slope is equal to the Lyapunov exponent λ . The exponent is included next to the label or series name, and it should be consistent throughout each plot for α_D .

2 Poisson Equation for Dipole

A grid was created such that the spacing between grid points is assumed to be 0.1. Two point charges of positive or negative one placed in the middle of the grid and are separated by 0.6 or by 6 grid points. There is a spherical boundary condition such that $V(R) = 0$, at a large distance such as when $R = 5$. This means that the point charges affect a circle of 50 grid points from the origin, and outside of this range the point charge effect becomes negligible.

The first approach to the problem, is to set up a grid and place the charges followed by applying the Jacobi relaxation algorithm with an appropriate tolerance and grid density. Each grid point is the average of its nearest neighbor grid points, which creates a blur-like effect. Figure 5 is the resulting plot with equipotential lines. It can be seen that the lines diminish in magnitude and stop being formed when outside of the initial condition of $R = 5$. This is consistent with the large-distance behavior of the dipole potential, which is that with increasing distance from a point charge, the dipole will decreasingly affect the space.

To investigate how the number of required iteration steps, N_{iter} , increases with reducing the tolerance error limit, ϵ , a plot of $N_{iter}(\epsilon)$ was made. The resulting plot is found in Figure 5. The relationship is that of the reciprocal function, meaning that a smaller tolerance will lead to more iterations.

The next implementation uses the Simultaneous Over-Relaxation Method (SOR). This method uses both the updated grid while traversing and the old grid

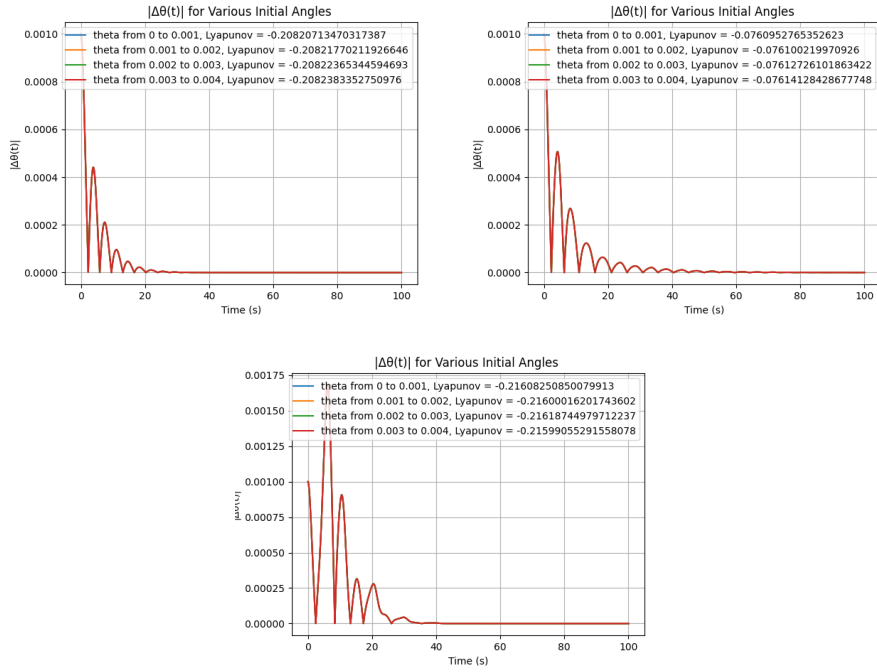


Figure 4: Difference in simulation using Runge-Kutta 4th order method used for finding θ where $\Delta\theta$ varies by 0.001 rad.

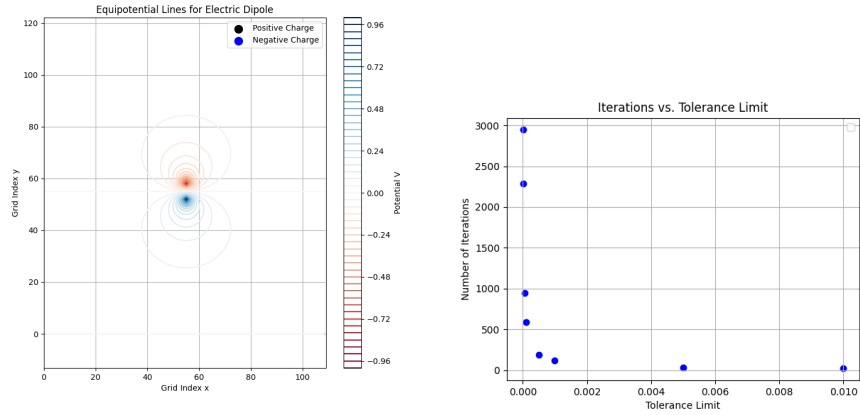


Figure 5: Poisson's Equation using the Jacobi relaxation algorithm(left) and Jacobi Iterations vs. Tolerance (right).

to improve runtime. To compare the two methods, the number of iterations was compared for the number of grid points. Theoretically, N_{iter} is proportional to n^2 for the Jacobi method and proportional to n for SOR. The results are shown on Figure 6. It is visible that the Jacobi method does increase in iterations as the grid number or grid dimension increases. It is possible that the proportionally through n^2 is not visible due to the small sample being taken or due to using an incorrect tolerance. The SOR method slightly increases in iterations with an increase in grid number, however, the proportionality with n is not necessarily visible. This may be due to the small sample size.

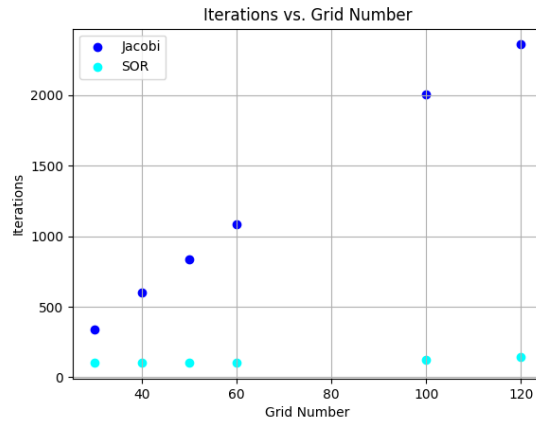


Figure 6: Grid dimension n vs. Iterations of Jacobi and SOR.